OPTO-ELECTRONICS REVIEW 8(4), 388–392 (2000)

Photosensitive macroporous silicon based structures

V. PAČEBUTAS[1*], K. GRIGORAS[1], V. JASUTIS[1], S. KAČIULIS[1,3], S. MICKEVIČIUS[1], J. SABATAITYTĖ[1], V. SNITKA[2], and I. ŠIMKIENĖ[1]

[1]Semiconductor Physics Institute, 11 Goštauto Str., 2600 Vilnius, Lithuania
[2]Research Center "Vibrotechnika", Kaunas University of Technology, Lithuania
[3]CNR-ICMAT, P.O. Box 10, 1-00016, Monterotondo Scalo, Rome, Italy

Macroporous silicon prepared in n-type silicon have been used for a photosensitive device formation. Boron-doped spun-on layer was applied for p^+ emitter formation of the devices. The obtained structures were investigated by AFM and electron microscopy, photosensitivity and the photocurrent spectra were measured to evaluate the influence of porous layer and boron diffusion conditions. Unusually fast boron diffusion through the porous emitter was investigated, stipulating the p^+-n junction to be positioned 2.5 μm deeper the pores bottom. This effect was explained by a presence of local electric fields, caused by tensions present at the border between PS layer and crystalline substrate and by possible deeper nanoporous structure, what was partially proofed by AFM.

Keywords: porous silicon, macropores, boron diffusion, photodetectors.

1. Introduction

The interest in porous silicon (PS) caused by observation of its unusual luminescence [1] is not diminishing till now. Quite the contrary, different papers show even new successful applications of this material in: photonic crystals [2], LEDs [3,4], sensors [5,6], spectrometry [7], microelectromechanical systems (MEMS) [8,9], solar cells [10,11]. In every special case, a porous silicon with different type of pores can be exploited from nanopores (< 2 nm) and mesopores (2–50 nm) to macropores (> 50 nm) [12].

Great variety of porous silicon based devices requires not only good skills in PS preparation. In most cases of device fabrication ohmic contacts are necessary [13], and doping of the layer, before or after the electrochemical etching procedure must be performed [14]. The p-n junction characteristics are very important in a solar cell performance so, attempts to incorporate the porous silicon emitter here requires knowledge of doping process through this layer. Several techniques have been used trying to exploit the enhanced surface area and the light trapping effect in macroporous silicon: doping from a solid source [15], doping from liquid films deposited by a spin-on technique [16]. Diffusion from spin-on glasses is simple enough from technological point of view, although the mechanism of such diffusion has not been fully understood yet [17]. Optimal emitter porosity and diffusion parameters must be evaluated in this case.

In this work, the samples with a PS layers, having typical pore dimensions and depth of some micrometers (macroporous silicon), were prepared trying to employ their light trapping action for a photodetectors improvement. Thick macroporous emitter was formed by boron doping from spin-on glasses prepared from organic solution. Electron and atomic force microscopy (AFM), X-ray photoelectron spectroscopy (XPS), photosensitivity and photocurrent spectra measurements were performed in order to investigate boron diffusion into porous structures and to evaluate the dependencies of photodetector performance on PS and emitter doping preparation conditions.

2. Sample preparation

The samples for etching were sliced from one-side polished, (100)-oriented, n-type silicon wafers (CZ) of specific resistivity of 1 Ω cm. They were initially cleaned by boiling for 10 min in dimethylformamide and in acetone, the native oxide layer was removed rinsing in HF. The PS layers were prepared by electrochemical etching the samples in HF: ethanol (1:1) electrolyte for 5 or 15 min under 30, 50, or 70 mA/cm^2 current densities. A simple home-made teflon etching cell with a rubber frame gasket was used [18]. 100 W halogen lamp was used for the front side illumination during the etching. The etched area was about 2 cm^2. The nanometer size, top part of prepared PS was removed in KOH solution. Remaining part of the PS layer was sponge-like with dimensions of the voids and the columns of some micrometers. The layer thickness was 2–12 μm. The samples were then dried in ambient air.

* e-mail: vaidas@opel2.pfi.lt

A spin-on technique was applied for the p^+-n junction formation. A boron oxide (B_2O_3) solution in tetraethoxysilane $Si(OC_2H_5)_4$ (TEOS) was used as a boron source. For some samples, boron oxide was diluted in ethyl alcohol and then mixed with TEOS, to increase its wetting character of solution. In both cases, concentration of B_2O_3 was 30%. The spun-on layers were dried for one hour at 300°C. Boron diffusion was performed by annealing the samples in argon ambient for 1 hour at 1100°C [16]. The borosilicate glass (BSG) was etched away in a buffer hydrofluoric acid (BHF) solution.

For a comparison, polished not etched samples were also prepared the same way in order to define peculiarities of boron diffusion into porous silicon. The characteristics of the samples, used for XPS measurements are listed in Table 1.

The sample photodetectors were made by slicing the inner 1 cm^2 area of the sample to prevent the possible electric shortenings at the edges. The contacts for photodetectors were prepared by evaporation of chromium/silver layer on the back, and by depositing of silver paste grid on the front surface. The contacts have been not annealed.

3. Investigation of porous emitter

3.1. Boron diffusion

The optimum emitter formation could correspond to the junction laying some deeper than the pores, and with twisted shape-repeating the pores bottom [11], increasing the active area this way.

Planar and cross-sectional surfaces of our samples were investigated by a scanning electron microscope (SEM) BS300 in the electron beam induced current (EBIC) mode and in the secondary electron image mode (with primary beam energy till 26 keV). The EBIC technique and electrochemical staining of the junction were applied for emitter thickness evaluation. Both techniques indicated that p^+-layer is some μm deeper than the pores are penetrating (Fig. 1). Very similar results were obtained for the samples etched at different conditions: the junction was about 2.5 μm deeper the pores bottom, irrespective of the PS thickness. This can mean that BSG deposited by spin-on technique penetrates well into the pores, and boron diffusion starts just at the pores walls and bottom places. Surprising enough is deep penetration of boron: the junction prepared at the same conditions into polished sample was only about 1 μm depth. From other side, this value is also high enough, because standard boron diffusion from gas-phase with annealing for 1 hour at 1100°C would give a p^+-n junction of approximately 0.4-μm depth. In our experiments, doping from BSG prepared by spin-on technique leads to junction depths of 1 μm and 2.5 μm for polished and porous samples, respectively. Enhanced boron diffusion in Si during doping from borosilicate glass have been reported elsewhere [19], stating that native oxide between BSG and Si affects the doping characteristics a great deal. In our experiments, the native oxide, which could form a barrier for boron diffusion, is dissolving into liquid BSG at high temperature.

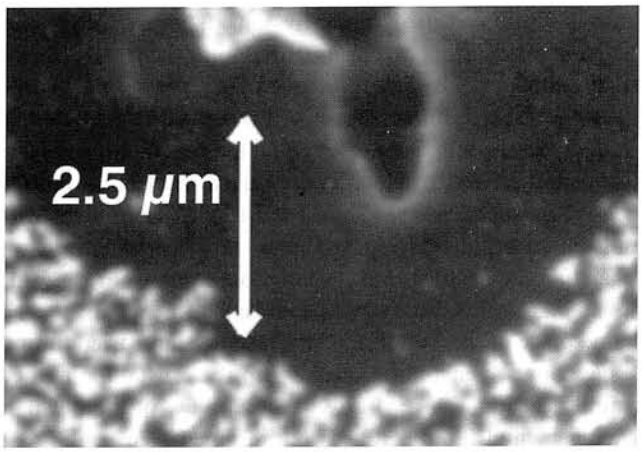

Fig. 1. SEM cross-section view of porous emitter with electrochemically stained p-n junction position (PS formed by etching for 15 min under 70 mA/cm^2).

In the case of porous emitter, obtained deep p^+-n junction (Fig. 1) could confirm the statements that PS can significantly increase the diffusion of impurity into silicon [20]. From other side, the junction, found 2.5 μm deeper than the porous layer reaches, indicates that enhanced diffusion of boron takes place behind the PS layer – in crystalline silicon. Two explanations seem to be reasonable here. First of all, a nanoporous layer, which could lay behind the macro-PS could act as a channel for diffusion. Secondly, local electric fields, caused by tensions present at the border between PS layer and crystalline substrate, can occur,

Table 1. Sample preparation conditions.

Sample No.	Liquid solution for doping	Annealing conditions	Layer for doping	Surface
1	30% B +C_2H_5OH	1100°C 1 h	BSG etched away	crystalline
2	30% B +C_2H_5OH		dried	crystalline
3	30% B+SiO_2	1100°C 1 h	BSG etched away	crystalline
4	30% B+SiO_2		dried	porous, 6 μm
5	30% B+SiO_2	1100°C 1 h	BSG etched away	porous, 6 μm

stimulating the drift of impurity ions. These tensions can become even stronger during the doping step because of high temperatures.

Atomic force microscope (AFM) technique was used to investigate the bulk area just behind the macroporous layer. The same sliced sample edges, as used in electron microscope measurements (Fig. 1), were tested. The main difficulty is just identifying the area of observation. After changing the cantilever tip, when proceeding from 2×2 μm^2 to 200×200 nm^2 area, it was impossible to remain on the same place of the sample. In any case, we have tried to find a nanopores, penetrating deeper into the crystalline part of emitter. In Fig. 2, AFM cross-section view of emitter part laying behind the macropore is presented. We could consider five parallel channels (darker areas in Fig. 2) as pores penetrating into the depth. Their characteristic diameters are 5–10 nm. It is only the preliminary result at present.

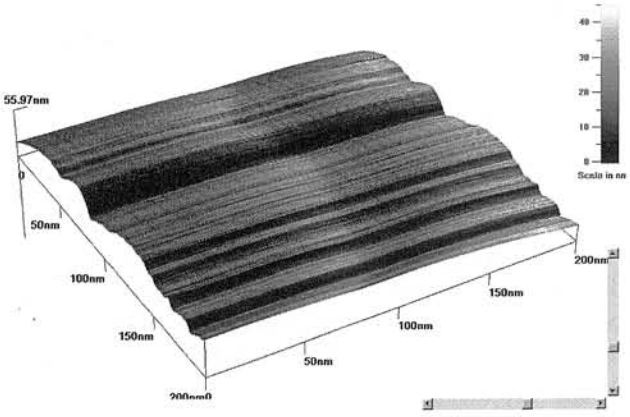

Fig. 2. AFM cross-section view of emitter area behind the macropore.

3.2. Boron concentration

Both the emitter thickness and doping level are important for a photosensitive device performance. Higher doping can increase the barrier high of p-n junction, but higher concentration leads also to higher surface recombination velocity, what reduces the photocurrent.

The concentration of boron at the surface was evaluated both in the spun-on film deposited for boron diffusion and in the obtained emitter, after the BSG removing. First of all, the sharp contrast obtained after the junction staining during the boron diffusion measurements confirmed high doping of emitter region. More detailed quantitative measurements were performed by XPS technique. Surface chemical composition of the samples was studied by the selected area X-ray photoelectron spectroscopy (SAXPS) in a VG ESCALAB MkII. The binding energy (BE) scale was calibrated by using C 1-s peak. Accuracy of the measured BE was +0.1 eV. A least-square routine of peak-fitting was used for XPS spectra analysis. The relative concentrations of chemical elements were calculated by using quantification routine, including Wagner's energy dependence of attenuation length and a standard set of the VG Escalab elemental sensitivity factors. Table 2 presents the BE values of the main XPS peaks and relative chemical composition of the investigated samples (the sample numbers are the same as in Table 1). All samples contain oxygen (in SiO_2 and as a contaminant), silicon (also in SiO_2, for annealed samples), carbon (as a contaminant). Unfortunately, the boron concentration in the samples with PS layer was to low for a present sensitivity of our XPS apparatus. Most probably, the complicated surface structure with voids and columns hindered the normal penetration of the X-beam. Also strange coincidence, Cl and Cr contaminants have not been detected in porous samples (Table 2), but we cannot state here any connections with boron. XPS data showed low presence of boron in all crystalline samples. At the same time, less boron was detected before diffusion, into spun-on layer (sample #2). This can be caused by some type of oxides formed during drying. Samples with this dried layer (#2, #4) contained much more oxygen (Table 2). After diffusion, the boron amount increases, and any big difference was observed for both compositions of the doping solution (samples #1 and #3). Typical XPS spectra are shown in Fig. 3. Experimental curve and fitting with some calculated peaks are presented. All peaks of silicon are very strong, so even peak of the second plasmon from Si 2s peak shadows a small B 1s peak. Anyhow, presence of boron confirms also Auger peak (not shown in this figure). Returning to Table 2, even after BSG etching, some amount of SiO_2 exists on the surface (samples #1, #3, #5). This can be attributed to the native oxide layer. From all detected elements it is possible to calculate the boron percentage and then, concentration. For sample #3 this value is 2.9%, what corresponds to 1.4×10^{21} cm^{-3}. This result shows that a highly doped emitter was prepared.

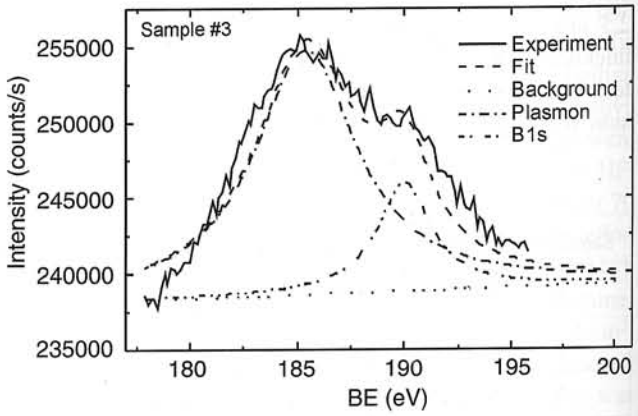

Fig. 3. XPS spectra for sample #3. Region with a shaded boron peak is presented. The inlet shows Auger peak (B KLL) also confirming boron presence.

Table 2. Binding energy (BE) values of the main XPS peaks and relative chemical composition (normalised to Si value) of the investigated samples.

Sample No.	Elements	O 1s	Si 2p		B 1s	Cl 2s	Cr 2p	C 1s
			Crystalline	In SiO_2				
	Average BE, eV	532.6	100.6	102.5	190.1	268.2	579.3	284.6
1	Atomic ratio	1.7	1.0	0.4	0.1	0.01	0.14	0.87
2		2.16	1.0	–	0.04	0.11	0.07	0.54
3		1.56	1.0	0.31	0.115	0.007	0.11	0.97
4		2.2	1.0	–	–	–	–	0.91
5		1.9	1.0	0.67	–	–	–	1.2

3.3. Photosensitivity

PS thickness and junction depth must influence the photosensitivity and photocurrent spectra of the sample detectors due to the different absorption and surface recombination conditions. Photocurrent dependence on the electrochemical etching current density is shown in Fig. 4. Sample surface was excited with a helium-neon laser beam (wavelength of 633 nm). All PS layers were prepared during etching for 15 min. Increase in photocurrent is clear for the samples prepared at lower current densities. It can be explained by thinner PS layer and its smoother structure. The junction position is much closer to the sample surface in this case what minimises the losses due recombination. From other side, the light trapping conditions must be quite similar at this wavelength for different samples (most macropores were of larger size than wavelength).

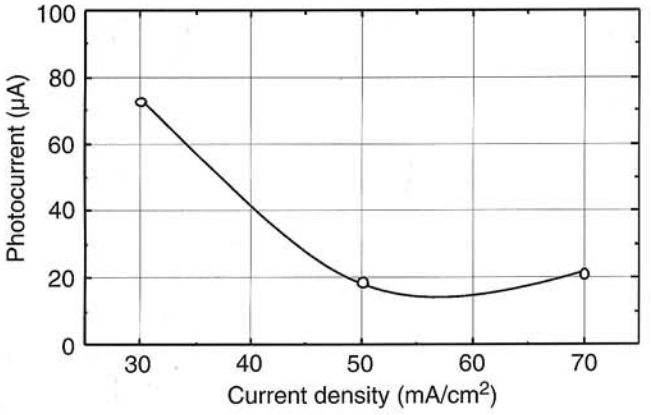

Fig. 4. Photocurrent dependence on electrochemical etching current density. Excitation with helium-neon laser.

Photocurrent spectra measured for the samples with a different PS layers are shown in Fig. 5. All the photocurrent spectra exhibit the maximum which position depends on the etching conditions. The sample with a thinnest PS (~ 0.4 μm, 5 min under 30 mA/cm²) has the maximum at about 670 nm. It shifts to the longer wavelengths by increasing etching duration and current density, reaching 780 nm for the thickest

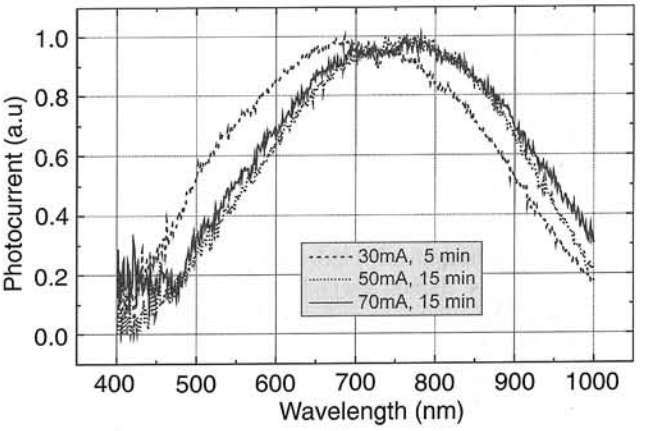

Fig. 5. Photocurrent spectra measured for the samples with different PS layers.

layer (~6 μm, 15 min under 70 mA/cm²). Such shift can be explained by absorption of short-wavelength photons in the regions between pores. In the case of thicker PS, those regions are deeper, and generated charge carriers must diffuse longer way to reach the junction area and can recombine with a higher probability, so, the photocurrent is lower at shorter wavelengths in this case.

4. Conclusions

Macroporous silicon layer was used as an emitter for photodetectors. Boron doped glasses deposited by spin-on technique were applied to form p^+-n junctions into macroporous structures. The junctions were found to lay about 2.5 μm deeper than the pore bottom, rather independently on the PS thickness. Enhanced boron diffusion was explained by a presence of local electric fields, caused by tensions present at the border between PS layer and crystalline substrate, which are stimulating the diffusion of impurity. Possible presence of nanoporous layer just behind the macropore bottom was checked by XPS, as an additional channel for faster boron diffusion. Photocurrent measurements showed a clear sensitivity dependence on the PS layer preparation conditions.

Reference

1. L.T. Canham, "Silicon quantum wire array fabrication by electrochemical and chemical dissolution of wafers," *Appl. Phys. Lett.* **57**, 1046–1048 (1990).
2. U. Grüning and V. Lehmann, "Two-dimensional infrared photonic crystal based on macroporous silicon," *Thin Solid Films* **276**, 151–154 (1996).
3. P.M. Fauchet, J. Behren, K.D. Hirschman, L. Tsybeskov, and S.P. Duttagupta, "Porous silicon physics and device applications: a status report," *Phys. Stat. Sol. (a)* **165**, 3–13 (1998).
4. S. Lazarouk, P. Jaguito, and V. Borisenko, "Integrated optoelectronic unit based on porous silicon," *Phys. Stat. Sol. (a)* **165**, 87–90 (1998).
5. A. Motohashi, M. Ruike, M. Kawakami, H. Aoyagi, A. Kinoshita, and A. Satou, "Identification of water molecules in low humidity and possibility of quantitative gas analysis using porous silicon gas sensor," *Jpn. J. Appl. Phys.* **35**, 4253–4256 (1996).
6. J. Sim, S. Halm, J, Lee, J. Lee, I. Yu, and L. Kim, "Eight-beam piezoresistive accelerometer fabricated by using a selective porous silicon etching method," *Proc. Int. Conf. Solid-State Sensors and Actuators (Transducers'97)*, Chicago, June 16-19, 1193–1196 (1997).
7. J. Wei, J.M. Buriak, and G. Siuzdak, "Desorption-ionisation mass spectrometry on porous silicon," *Nature* **399**, 243–246 (1999).
8. T. Bischoff, G. Müller, W. Welser, and F. Koch, "Frontside micromachining using porous-silicon sacrificial-layer technologies," *Sensors and Actuators A* **60**, 228–234 (1997).
9. R.W. Tjerkstra, J.G.E. Gardeniers, M.C. Elwenspoek, and A. Berg, "Electrochemical fabrication of multi walled micro channels," *Proc. μTAS'98 Workshop*, 133–136 (1998).
10. L. Stalmans, J. Poortmans, H. Bender, M. Caymax, K. Said, E. Varzsonyi, J. Nijs, and R. Mertens, "Porous silicon in crystalline silicon solar cells: a review and the effect on the internal quantum efficiency," *Prog. Photovolt. Res. Appl.* **6**, 233–246 (1998).
11. V.Y. Yerokhov, I.I. Melnik, and O.I. Iznin, "Photoconversion in solar cells structures with porous silicon," *Proc. SPIE* **3580**, 168–177 (1998).
12. U. Gösele and V. Lehmann, "Porous silicon quantum sponge structures: formation mechanism, preparation methods and some properties," *in Porous Silicon,* pp. 17–39, edited by Z.C. Feng and R. Tsu, World Scientific, Singapore, 1994.
13. J. Linnros and N. Lalic, "High quantum efficiency for a porous silicon light emitting diode under pulsed operation," *Appl. Phys. Lett.* **66**, 3048–3050 (1995).
14. S. Barret, F. Gaspard, R. Herino, M. Ligeon, F. Muller, and I. Ronga, "Porous silicon as a material in microsensor technology," *Sensors and Actuators A* **33**, 19–24 (1992).
15. R. Gamboa, M. Martins, J.M. Serra, J.M. Alves, A.M. Vallera, E.A. Ponomarev, and C. Levy-Clement, "Rirst solar cell on electrochemically textured macroporous silicon," *Proc. 2nd World Conf. Photovoltaic Solar Energy Conversion*, 6-10 July, Vienna, 1669–1672 (1998).
16. K. Grigoras, J. Härkönen, V. Jasutis, A. Kindurys, V. Pačebutas, J. Sabataitytė, and I. Šimkienė, "Porous silicon emitter formation from spin-on glasses", *Proc. 2nd World Conf. Photovoltaic Solar Energy Conversion*, 6-10 July, Vienna, 1717–1720 (1998).
17. K. Waczynski, E. Wrobel, and Z. Pruszowski, *Electron Technology* **30**, 138 (1997).
18. K.Grigoras and V. Pačebutas, "Porous silicon fabrication technique for large area devices," *Rev. Sci. Instrum.* **67**, 2337–2338 (1996).
19. M. Miyake, "Enhanced diffusion of boron in Si during doping from borosilicate glass", *J. Electrochem. Soc.* **154**, 2534–2538 (1998).
20. G. Amato, L. Boarino, N. Brunetto, and M. Turnaturi, "Deep 'cold' junctions by porous silicon impregnation," *Thin Solid Films* **297**, 321–324 (1997).

